

# Anthraquinone Azo Dye as a Novel Electrochemical Platform for the Simultaneous Detection of Dopamine and Serotonin: Synthesis and Characterization

K. M. Pallavi<sup>a</sup>, G. P. Mamatha<sup>a,\*</sup>, Pampapathi Shekharagouda<sup>a</sup>, and Chethan Krishnamurthy<sup>b</sup>

<sup>a</sup> Department of Studies in Chemistry, Davangere University, Davangere, Karnataka, Shivagangothri, 577007 India

<sup>b</sup> Department of Chemistry, Kuvempu University, Jnana Sahyadri, Shivamogga, Karnataka, Shankaraghatta, 577451 India

\*e-mail: mamathagpgp2020@gmail.com

Received December 7, 2023; revised February 21, 2024; accepted March 6, 2024

**Abstract**—A novel electrochemical sensor was designed by using a synthesized anthraquinone azo dye-based glassy carbon electrode was fabricated and used for enhanced selective determination of Dopamine (DA) and serotonin (5-HT) simultaneously at an optimum working potential (0.11 V for DA and 0.27 V for 5-HT). Utilizing spectroscopic techniques like FT-IR, HR-MS, and <sup>1</sup>H-NMR, a synthesized azo dye molecule structure was characterized. Different electrochemical techniques, including cyclic voltammetry (CV) and differential pulse voltammetry (DPV), were employed to study the electrochemical sensing abilities of the modified working electrode. The DA and 5-HT linear response ranges between current intensities and concentration were found to be 0.001–0.055 and 0.01–1.15 μM and the lower limit of detection (LOD) was 1.9 and 4.16 nM respectively. Further demonstrating the constructed electrochemical sensor's practical application were tests of reproducibility, stability, and real sample analysis with excellent recovery.

**Keywords:** anthraquinone azo dye, electrochemical sensor, dopamine, serotonin, real sample

**DOI:** 10.1134/S1023193524700289

## INTRODUCTION

In order to facilitate the transmission of information throughout the brain and body, neurotransmitters (NTs), which are endogenous chemical substances, serve as signal transducers between neurons or neurons and non-neuronal somatic cells through chemical synapses. These essential substances can be produced by several glands, including the adrenal, pineal, and pituitary glands. NTs are eventually gathered at neuronal terminals after being naturally stored in vesicles. The biogenic amines (NTs) that include serotonin, epinephrine, norepinephrine, dopamine, and amino acids (mostly tyrosine and acetylcholine) may be the most significant among them [1, 2].

In recent days electrochemical sensors are considered as an excellent tool in scientific research for detecting NTs (DA and 5-HT). can serve as helpful resources for the biomarkers of the disease. Compared to other traditional approaches, these sensors are reproducible, portable, affordable, and offer accurate, quick, and real-time analysis. With the use of advanced, effective materials, electrochemical sensors

help in the early and successful clinical monitoring, and diagnosis of diseases [3–5].

One of the most significant naturally occurring catecholamine neurotransmitters is dopamine (DA), which is crucial for the proper functioning of the hormonal, renal, and central neurological systems [6]. Additionally, DA regulates several physiological processes, including mental cognition, locomotion, emotion, learning, and memory [7, 8]. However, abnormal DA levels have been linked to neurological diseases like Parkinson's, senile dementia, and schizophrenia [9]. Hence it is crucial to estimate dopamine quantitatively.

The electroactive indolamine compound Serotonin (5-hydroxytryptamine) functions as a vasoconstrictor and neurotransmitter. It facilitates signal transmission that controls several biological processes and releases a substance in the brain that promotes mood [10, 11], and also plays a pivotal role in regulating physiological activity such as mood, sleep, emesis (vomiting), sexuality, and helps to manage hunger. Moreover, it supports the body's bowel movements and blood coagulation [12, 13].

The US Department of Health, Human Services, and National Institutes of Health (NIH) have published that the normal human serotonin level is 0.25–0.74  $\mu\text{M}$  [14]. Severe mental sicknesses like panic attacks, sadness, insomnia, stress, and inexplicable irritability are all related to low 5-HT levels. Elevated concentrations may cause toxicity and potentially lethal side effects include obsessive compulsive disorder, autism, and serotonin syndrome [15]. Hence quantification of 5-HT level is crucial for both diagnosing diseases associated with 5-HT and understanding its function in disorders related to neurons [16]. Hence, the development of electrodes for the simultaneous electrochemical detection of DA and 5-HT in a biological system has attracted focus from researchers. Since these NTs usually coexist in biological systems and exhibit close oxidation potential, mutually affect one another's release, and their relative concentrations have an impact on a variety of illnesses and how efficiently drugs work as treatments [17]. A few publications about the simultaneous detection of DA and 5-HT in the presence of Ascorbic acid (AA) using different electrodes and electrochemical techniques can be found in the literature. However, the presence of AA at a high concentration, which causes an overlapping voltammetric response, is a significant barrier to the simultaneous measurement of DA and 5-HT [15].

Recently, electrochemical polymerization of dye is the most influential method of depositing a conducting polymer layer which has a lot of interest in polymer-modified electrodes (PMEs) due to the high adhesion of polymer films to the electrode surface, as well as their good stability, reproducibility, and abundance of active sites during electrochemical deposition [18, 19]. Since electropolymerization is a better method to immobilizing polymers to prepare PMEs. Which supports the electrochemical parameters to control charge transport characteristics, film thickness, and permeation. Generally, carbon-base electrodes have been utilized; of these, bare glassy carbon electrodes (BGCE) is utilized more frequently than metal electrodes because of their biocompatibility with tissue, low residual current across a broad potential range, and low tendency to exhibit a deteriorated response as a result of electrode fouling [20–23]. Moreover, the electropolymerization approach overcomes solubility challenges that are frequently complicated in other methods. Also, electropolymerization is a simple and less expensive process compared to other modifying procedures, simply the corresponding monomer is dissolved and the polymeric layer is directly formed on the conducting electrode surface [24, 25].

There are several drawbacks to using typical electrodes for simultaneous electrochemical measurement

of DA and 5-HT, including large overpotentials, sluggish electron-transfer processes [26, 27], and poor sensitivity and reproducibility. These drawbacks can be solved through synthesized novel anthraquinone mono-azo dye named ((4-aminophenyl)diazinyl)anthracene-9,10-dione (ADA) modified electrode was prepared by electropolymerization method. Which also makes an excellent material for glassy carbon electrode modification. To the best of our knowledge, no prior reports have been made about the electropolymerization of ADA. Therefore, we present the electrochemical polymerization of ADA and its electrochemical characteristics for the first time in this study. The developed poly(p)-ADA/modified glassy carbon electrode (MGCE) demonstrated good stability after multiple cycles, and the simultaneous detection of DA and 5-HT in serum and urine samples was also accomplished.

## EXPERIMENTAL

### *Materials and Methods*

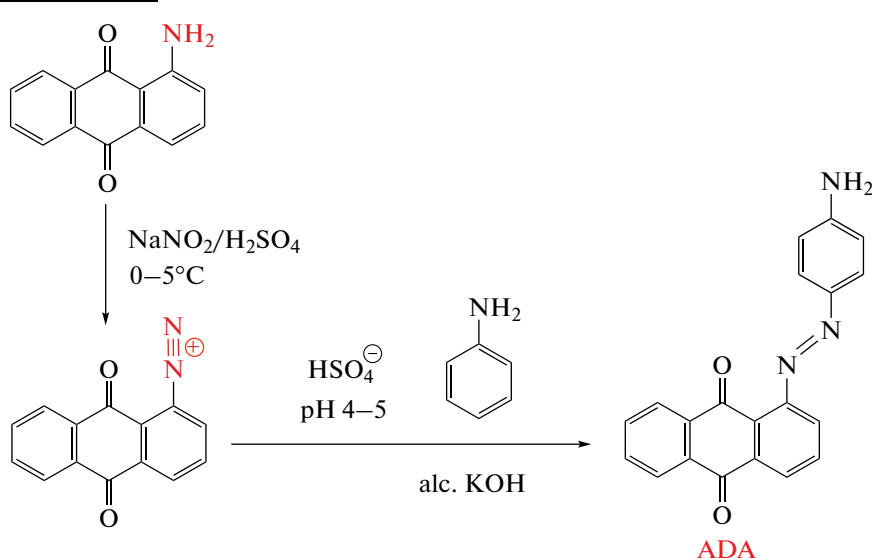
The 1-Amino-anthraquinone and coupling components were obtained from Sigma-Aldrich and were of analytical quality.  $^1\text{H-NMR}$  and FT-IR spectra were recorded by JEOL apparatus at 399.78 MHz instrument using deuterated dimethyl sulfoxide (DMSO) as a solvent and Bruker spectrometer respectively. The high-resolution mass spectral characteristics was recorded in waters USA Model-Xevo G2-XS QT of Instrument. All electrochemical studies were carried out on a CHI-660E voltammetric analyzer (CH-instrument-660E electrochemical workstation) with a conventional three-electrode system. Platinum wire, Ag/AgCl electrode and bare glassy carbon electrode and ADA modified glassy carbon electrode (BGCE and ADA/MGCE), as counter, reference and working electrodes respectively. All the experiments were performed at room temperature.

### *Synthesis of Anthraquinone Mono-Azo Dye*

2 mM 1-amino-anthraquinone (0.435 g) was slowly introduced into concentrated sulfuric acid (5 mL) and a solution of 2 mM  $\text{NaNO}_2$  (0.143 g) in Conc.  $\text{H}_2\text{SO}_4$  was taken in a round bottom flask. After stirring for 4 h at room temperature, and then it was quenched with ice water (60 mL). The diazonium salts were obtained by filtration of the mixture. The diazonium salt was added to 30 mL of water with 5 mL dilute hydrochloric acid and the mixture was stirred for 30 min. The ensuing mixture was dropped into a solution of aniline (0.186 g, 2 mM) dissolved in alcoholic KOH (10 mL) for the coupling reaction. In the course of dropping, the temperature and pH of the mixture were maintained at 0–5°C and 4–5 pH

respectively by adding saturated sodium bicarbonate, and the precipitate was collected by filtration. The product ((4-aminophenyl)diazinyl) anthracene-9,10-

dione (ADA) was washed with water and dried in a vacuum oven. Anthraquinone azo dye was synthesized as shown in Scheme 1.



Scheme 1. Synthetic route for the preparation of ADA.

#### Preparation of Real Samples

Without any prior pretreatment, 1 mL of the serum sample was added to a 100 mL volumetric flask containing a supporting electrolyte phosphate buffer solution (PBS) pH 7.0. This diluted solution was pipetted into series of 10 mL volumetric flasks. To this, a known standard concentration of DA and 5-HT solutions was added and diluted up to the mark with 0.2 M PBS (pH 7.0) [28].

Samples of urine were collected and immediately stored in a refrigerator. The 10 mL of the collected samples were centrifuged for 15 min at a speed of 2000 rpm. The supernatant was filtered, and different volumes of the filtrate were transferred into a 10 mL volumetric flask and diluted to the mark with 0.2 M PBS (pH 7.0), a series of known amounts of DA and 5-HT were spiked to the diluted urine samples [29].

## RESULTS AND DISCUSSION

### Electrochemical Characterization Fabrication of p-ADA/MGCE

Prior to modification, the glassy carbon electrode was polished with a 0.05 M alumina slurry after being successively sonicated many times with ethanol and water for two minutes. Several CV scans in 0.5 M H<sub>2</sub>SO<sub>4</sub> were used to activate until consistent voltammograms were obtained. Subsequently, the poly ADA film was electrochemically deposited in 0.2 M phos-

phate buffer solution (pH 7.0) containing 1 mM ADA monomer. The cycling potential of the solution was set to range from –0.5 to +1.5 V, with a scan rate of 50 mV s<sup>-1</sup>, for ten continuous cycles as shown in Fig. 1a by using the CV method. The electro-deposition process has confirmed the development of p-ADA membrane on BGCE, as evidenced by the peak current gradually increasing with increasing scan time. The thickness of the adhering polymer film directly influences the modified electrode's electrocatalytic performance. It is possible to effectively control the film thickness by varying the number of cycles (from 5 to 20 cycles) that are performed during the polymerization process, and the resulting DA and 5-HT peak current was measured Fig. 1b. Excellent catalytic sensitivity is demonstrated by the 10 cyclic sweeps for both DA and 5-HT. Therefore, ten cycles were chosen for further modification. The electrode surface was thoroughly washed with doubly deionized water after each modification to remove the untreated monomer molecule. The resulting electrode is abbreviated as p-ADA/MGCE.

### Redox Active Surface Area of BGCE and p-ADA/MGCE

A cyclic voltammetric technique was used to evaluate the charge transfer characteristics of the BGCE and p-ADA/MGCE by placing the electrodes in 2.5 mM K<sub>3</sub>[Fe(CN)<sub>6</sub>] in 0.1 M KCl. Figure 1c depicts

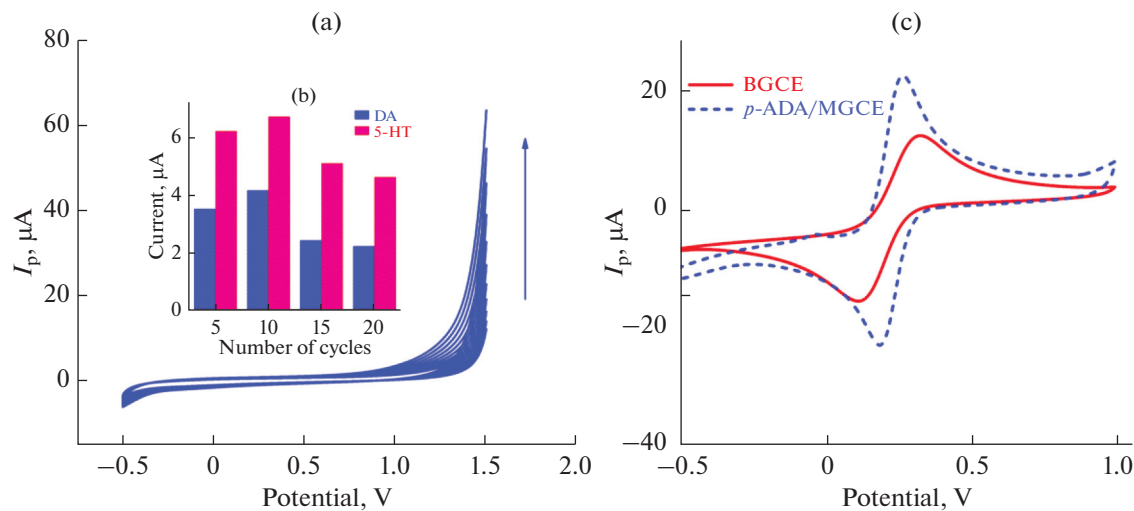


**Fig. 1.** CVs of polymerization of ADA in 0.2 M PBS (pH 7) on BGCE for 10 cycles in the potential range from  $-0.5$  to  $1.5$  V with a sweep rate of  $50 \text{ mV s}^{-1}$  (a). Plot of oxidation peak current of DA and 5-HT vs. polymerization segments (b). CVs of  $2.5 \text{ mM K}_3[\text{Fe}(\text{CN})_6]$  in  $0.1 \text{ M KCl}$  at p-ADA/MGCE (dashed curve) and BGCE (solid curve) with a sweep rate of  $50 \text{ mV s}^{-1}$  (c).

the cyclic voltammograms recorded at p-ADA/MGCE (dashed curve) and BGCE (solid curve) respectively. The redox peak separation ( $\Delta E_p$ ) values and anodic peak current are found to be  $0.213 \text{ V}$  and  $12.43 \mu\text{A}$  for BGCE and  $0.081 \text{ V}$  and  $22.5 \mu\text{A}$  for p-ADA/MGCE respectively. The peak current for the modified electrode dramatically increases when the redox peak separation value decreases. These results indicate increased electron transfer rate and electroactive sites. Randles–Sevick’s equation (1) is used to compute the active surface area of p-ADA/MGCE and BGCE utilizing the CV approach and data from the literature [30, 31].

$$I_p = (2.69 \times 10^5) n^{3/2} A D_0^{1/2} C^0 v^{1/2}, \quad (1)$$

where  $A$  is the area of the electroactive surface area ( $\text{cm}^2$ ),  $I_p$  is the peak current (A),  $n$  is the number of electrons participating in the redox reaction ( $n = 1$ ),  $D$  is the diffusion coefficient of the redox probe ( $12.2 \times 10^{-6} \text{ cm}^2/\text{s}$  for  $[\text{Fe}(\text{CN})_6]^{3-}$ ) [32],  $C$  is the concentration of the reactive species in the electrolyte ( $10^{-6}$  for ferri system  $\text{mol cm}^{-3}$  here), and  $v$  is the scan rate ( $\text{V s}^{-1}$ ). The calculated active surface area was found to be  $0.023 \text{ cm}^2$  for BGCE (3 mm diameter) and  $0.043 \text{ cm}^2$  for p-ADA/MGCE.

#### Catalytic Performance for DA and 5-HT at Different Working Electrodes

By facilitating the CV approach, the electrochemical analyses of the targeted analytes were examined at bare and modified electrodes. Figures 2a and 2b rep-

resents the cyclic voltammograms (CVs) recorded between  $-0.2$  to  $+0.6$  V in the absence of DA and 5-HT in  $0.2 \text{ M PBS}$  of pH 7.0 with a sweep rate of  $50 \text{ mV s}^{-1}$  at p-ADA/MGCE (dotted curve *a* and *d*), in the presence of  $0.1 \times 10^{-4} \text{ M}$  DA and  $0.5 \times 10^{-4} \text{ M}$  5-HT at BGCE (dashed curve *b* and *e*) and at p-ADA/MGCE (solid curve *c* and *f*) and small oxidation peak signals were seen for DA and 5-HT in the case of BGCE. The analytical signals of DA and 5-HT are significantly elevated and over potential is minimized with the electropolymerization of ADA onto the BGCE surface. This increase in peak current is ( $I_p 8.3 \mu\text{A}$  at  $E_p 0.18 \text{ V}$  for DA and  $I_p 59.7 \mu\text{A}$  at  $E_p 0.32 \text{ V}$  for 5-HT respectively) attributable to the enhanced catalytic efficiency and reactive sites of p-ADA/MGCE for the electro-oxidation of DA and 5-HT [33].

#### Effect of pH on DA and 5-HT Peak Current

pH of the electrolyte solution in which the reaction is occurring has a significant impact on the electrochemical investigations. The effect of pH on electro-oxidation of DA ( $0.1 \times 10^{-4} \text{ M}$ ) and 5-HT ( $0.5 \times 10^{-4} \text{ M}$ ) in different pH values (5.8–7.8) of  $0.2 \text{ M PBS}$  with sweep rate  $50 \text{ mV s}^{-1}$  at p-ADA/MGCE using CV technique has been studied. The Cyclic voltammograms for the reversible process of dopamine and irreversible oxidation of 5-HT are depicted in Figs. 3a and 3b respectively, which reveals that the peak positions shifted towards a greater negative potential as pH values increase. At pH 7.0, both DA and 5-HT show the maximum peak currents, hence pH 7.0 is considered as an optimum pH. The linear relationship obtained

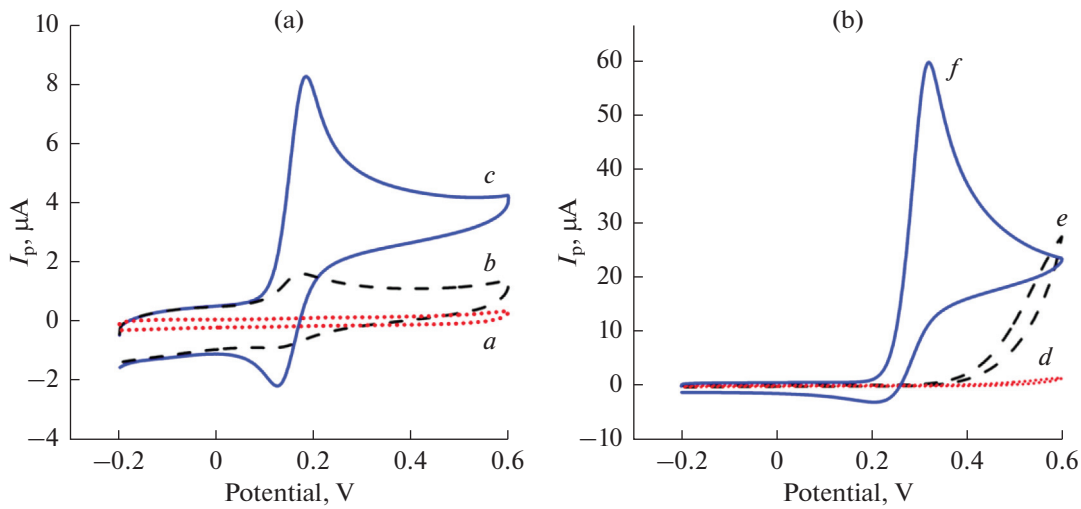


**Fig. 2.** CVs of  $0.1 \times 10^{-4}$  M DA (a) and  $0.5 \times 10^{-4}$  M 5-HT (b) in 0.2 M PBS (pH 7.0) with sweep rate of  $50 \text{ mV s}^{-1}$  at, BGCE (dashed curve b, e), and p-ADA/ MGCE (solid curve c, f) and CVs in the absence of DA and 5-HT at p-ADA /MGCE in 0.2 M PBS (dotted curve a, d) respectively.

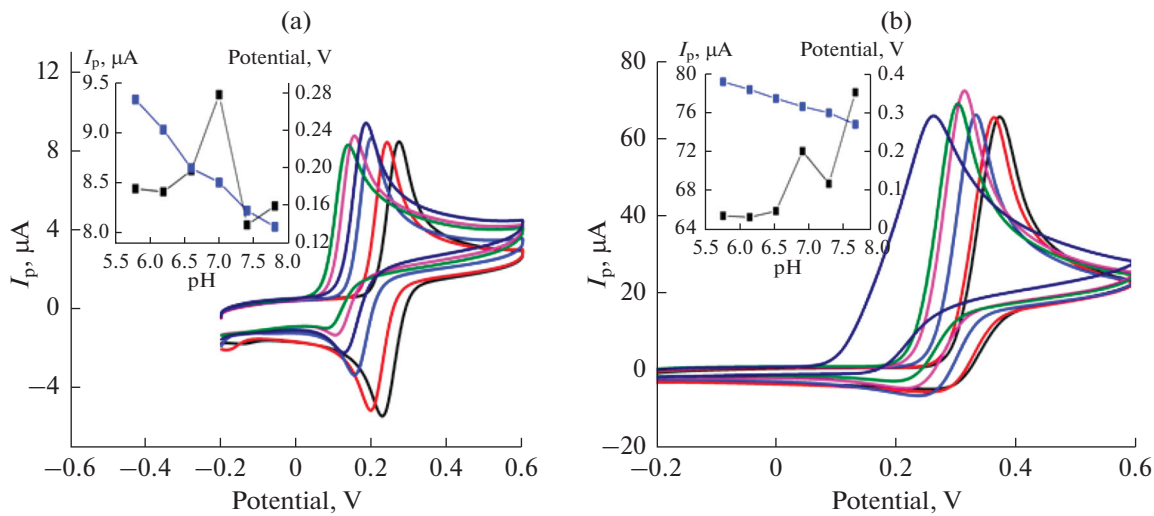


**Fig. 3.** CVs of  $0.1 \times 10^{-4}$  M DA (a) and  $0.5 \times 10^{-4}$  M 5-HT (b) recorded at p-ADA/MGCE in 0.2 M PBS of different buffer pH values (5.8–7.8) having the sweep rate of  $50 \text{ mV s}^{-1}$ . Inset: (a & b) Calibration plot of pH vs. obtained peak current vs. peak potential of DA and 5-HT respectively.

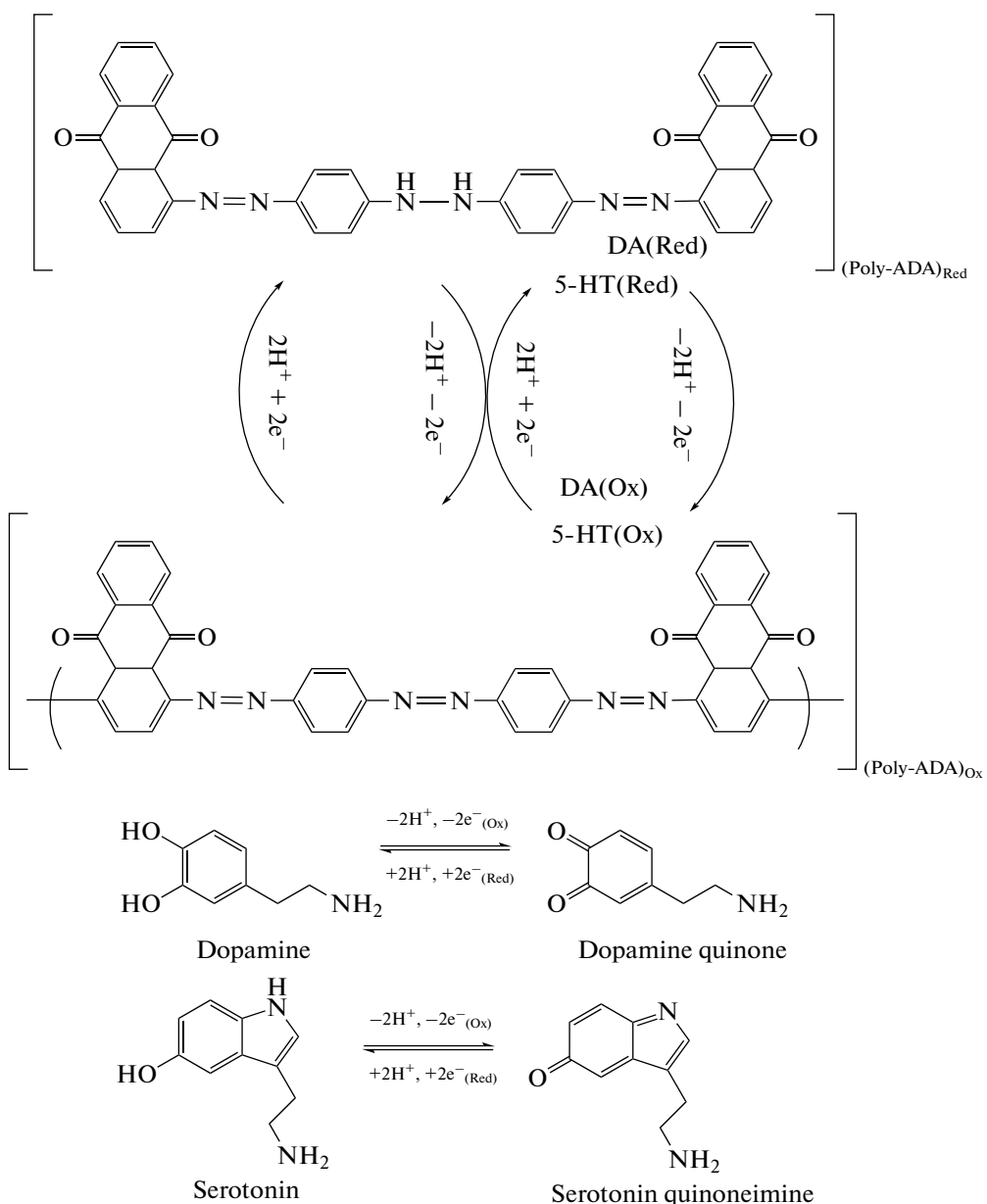
between the potential and pH is depicted in the insets of Figs. 3a and 3b for DA and 5-HT respectively with regression equations as follows:

$$E_p(\text{DA})/\text{V} = -0.0707\text{pH} + 0.6758 \quad (R^2 = 0.994)$$

and

$$E_p(5\text{-HT})/\text{V} = -0.053\text{pH} + 0.690 \quad (R^2 = 0.983).$$

The slopes, obtained at 0.070 and 0.053 V/pH, are in proximity to 0.059 V/pH, further manifesting that the number of electrons (two electrons) transported matched the number of protons (two H<sup>+</sup> ions) involved in the reaction [15, 34]. The mechanism of electrooxidation of DA and 5-HT with the participation of a synthesized ADA azo dye as a catalyst will be given in Scheme 2 [12, 34, 35].



**Scheme 2.** Mechanism for electrocatalysis of DA and 5-HT with the participation of p-ADA/MGCE.

#### Effect of Scan Rate at p-ADA/MGCE

Cyclic voltammetry technique was employed to analyze the kinetic characteristics of the reaction at the p-ADA/MGCE electrode and investigate the effect of the scan rate on the voltammetric response related to DA and 5-HT oxidation throughout a potential span of  $-0.2$  to  $0.6$  V. The peak current increased with an increase in the scan rate; this is because of the decrease in the size of the diffusion layer [3]. Figures 4a and 4b illustrate that the voltammograms of  $0.1 \times 10^{-4}$  M DA and  $0.5 \times 10^{-4}$  M 5-HT respectively in  $0.2$  M PBS (pH 7.0) solution at differ-

ent sweep rates ranging from  $50$ – $500$  mV s $^{-1}$ , clearly show that oxidation peak current increased with the sweep rate. As seen in Figs. 4a and 4b insets, a linear relationship is found between the logarithmic anodic peak current and the logarithmic scan rate, with linear regression equations expressed as follows

$$\log(I_p)(\mu\text{A}) = 0.438 \log(v)(\text{mV s}^{-1}) + 0.136;$$

$$R^2 = 0.987 \text{ for DA,}$$

$$\text{and } \log(I_p)(\mu\text{A}) = 0.367 \log(v)(\text{mV s}^{-1}) + 1.148;$$

$$R^2 = 0.986 \text{ for 5-HT.}$$

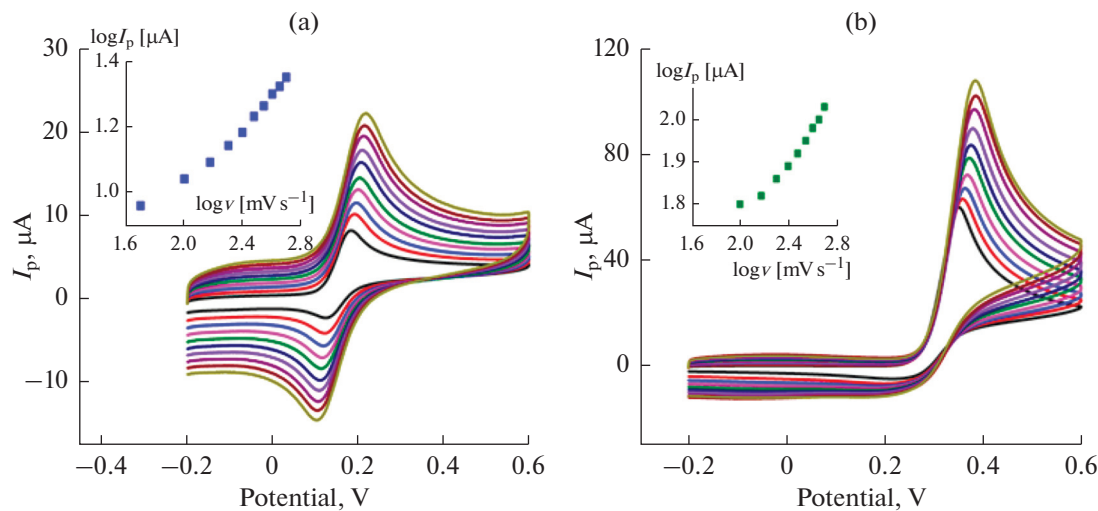


**Fig. 4.** CVs of  $0.1 \times 10^{-4}$  M DA (a) and  $0.5 \times 10^{-4}$  M 5-HT (b) in assistance with 0.2 M PBS of pH 7.0 with sweep rates (50–500)  $\text{mV s}^{-1}$  at p-ADA/MGCE. Inset: Plot of  $\log I_p$  of vs.  $\log v$ .

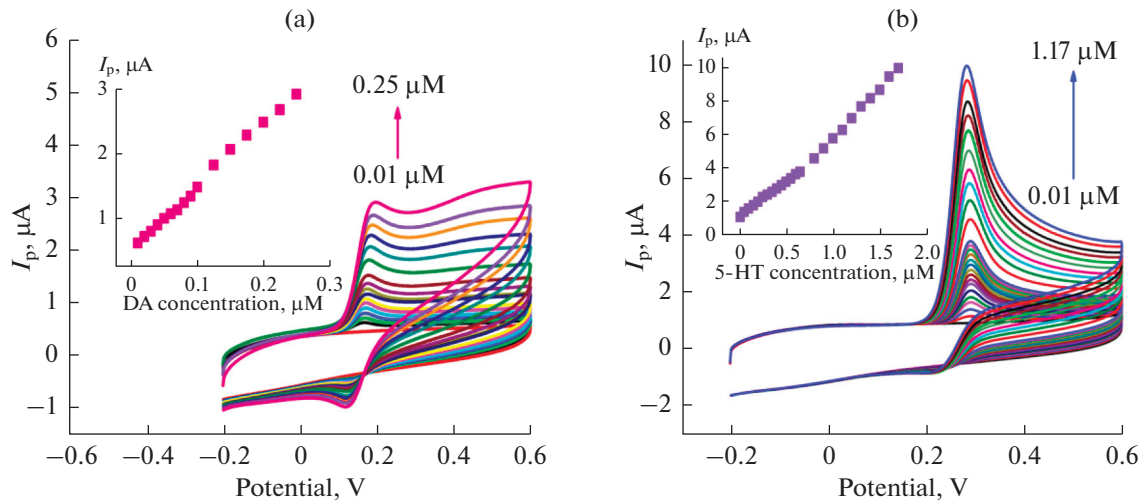


**Fig. 5.** CV curves obtained with different concentrations of DA on p-ADA/MGCE in 0.2 M PBS (pH 7.0) (a). Inset linear plot of current vs. DA concentration (0.01–0.25  $\mu\text{M}$ ) and CV curves on p-ADA/MGCE in 0.2 M PBS (pH 7) (b). Inset plot of  $I_{pa}$  and different concentrations of 5-HT (0.01–1.17  $\mu\text{M}$ ).

Since both experimental slopes will be closer to the anticipated value, which is equal to 0.5 for the ideal electrochemical reaction triggered by the diffusion-controlled process, it will be clear that the electrode behaviour was indeed a diffusion-controlled sensor process [16, 36].

#### *Detection Sensitivity of p-ADA/ MGCE for DA and 5-HT*

The quantification of DA and 5-HT was investigated by choosing both cyclic voltammetric and differential pulse voltammetric techniques.

**I. CV method.** The voltammetric performance of 5-HT and DA in altering their concentration has been evaluated to confirm the analytical efficacy. Figures 5a and 5b show the Cyclic voltammograms of various DA and 5-HT concentrations respectively. The peak oxidation current ( $I_p$ ) increased as the concentration of the analytes increased, according to the results. The calibration curve for DA (inset Fig. 5a), displayed a linear range from 0.01 to 0.25  $\mu\text{M}$  with the correlation coefficient  $R^2 = 0.9980$  and the linear equation  $I_p$  ( $\mu\text{A}$ ) =  $9.815$  ( $\mu\text{M}$ ) +  $0.484$ , similarly, inset Fig. 5b depicts the calibration plot of 5-HT showed a linear range from 0.01 to 1.17  $\mu\text{M}$ , the calibration plot of current versus 5-HT concentration exhibits linearity according to

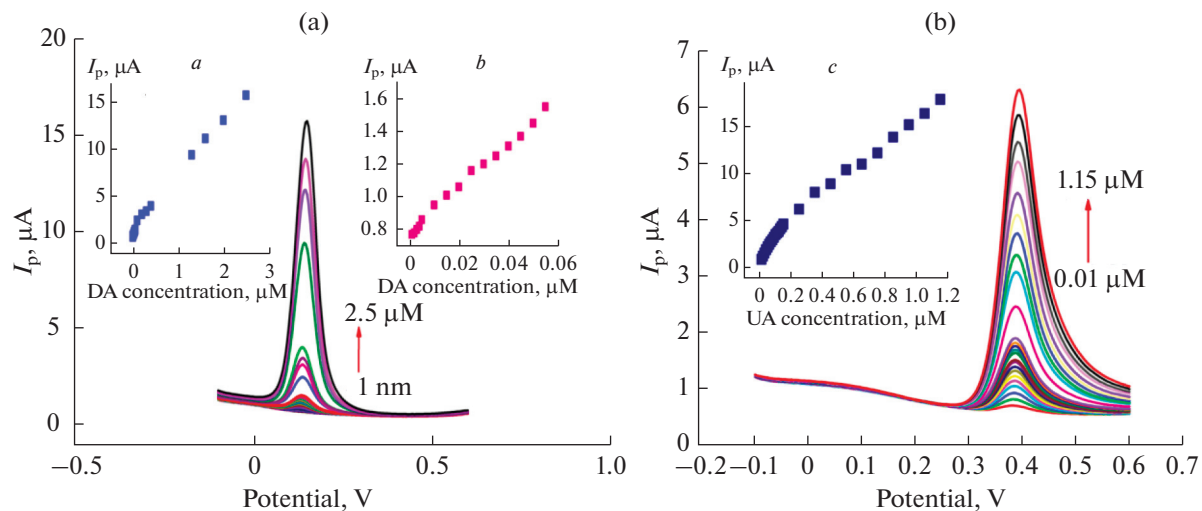


**Fig. 6.** DPV curves obtained with different concentrations of DA on p-ADA/MGCE in 0.2 M PBS (pH 7.0) (a). Inset (a) linear plot of current vs. DA concentration (1 nM–2.5 μM) and (b) is a calibration plot in low concentration of DA (0.001–0.055 μM). DPV curves on p-ADA/MGCE in 0.2 M PBS (pH 7.0) (b). Insert (c) is a plot of  $I_{pa}$  and concentration of 5-HT (0.01–1.15 μM).

regression equation:  $I_p(\mu\text{A}) = 5.2(\mu\text{M}) + 0.806$  ( $R^2 = 0.9961$ ) Limit of detection and quantification limits were proposed by using the formulae (2) and (3) respectively [37]. The estimated values of LOD and sensitivity were found to be 1.52 nM and 0.22 mA  $\mu\text{M}^{-1} \text{cm}^2$  for DA and 8.9 nM and 0.12 mA  $\mu\text{M}^{-1} \text{cm}^2$  ( $n = 5$ ) for 5-HT respectively.

$$\text{LOD} = 3S/M, \quad (2)$$

$$\text{LOQ} = 10S/M. \quad (3)$$

Here,  $S$  denotes the standard deviation and  $M$  is the slope obtained from calibration plots.

**II. DPV method.** Figures 6a and 6b show the differential pulse voltammetric curves for DA (1 nM–2.5 μM) and 5-HT (10 nM–1.15 μM) respectively, in 0.2 M PBS (pH 7.0) using the optimal DPV parameters: scan increment at 0.004 V and pulse amplitude of 0.05 V along with potential window –0.2 to +0.6 V. It was found that when the concentrations of DA and 5-HT increase, correspondingly the Oxidation peak current increases. The calibration curve between the  $I_p$  vs.  $C(\mu\text{M})$  was found to be linear, as shown in the inset of Figs. 6a and 6b, which gives the linear equations  $I_p(\mu\text{A}) = 13.74(\mu\text{M}) + 0.777$  ( $R^2 = 0.995$ ) and  $I_p(\mu\text{A}) = 4.758(\mu\text{M}) + 1.046$  ( $R^2 = 0.994$ ), respectively. The LOD and sensitivity obtained with the p-ADA/MGCE were 1.9 nM and 0.34 mA  $\mu\text{M}^{-1} \text{cm}^2$  for DA and 4.16 nM and 0.11 mA  $\mu\text{M}^{-1} \text{cm}^2$  ( $n = 5$ ) for 5-HT respectively. The developed electrochemical sensor will be useful for practical applications since the achieved detection limit value is less than the healthy human serotonin concentration level (0.25–0.74 μM) that has been approved by the US Department of Health and NIH [14]. The sensitivity of the electrode

and its lower detection limit indicated a considerable increase in the electroactivity of the ADA surface towards DA and 5-HT. A lower detection limit had been achieved as a result of the material's enhanced conductivity and electrocatalytic activity. The comparative analytical performance of DA and 5-HT for different modified electrodes, limit of detection, and methods used are tabulated in Tables 1 and 2 respectively.

#### Simultaneous Determination of DA and 5-HT

The oxidation potential of the electroactive biomolecule DA and 5-HT is extremely close to each other. Consequently, DA and 5-HT could potentially interfere significantly. DPV is more sensitive than CV since it was made to reduce the background capacitive current that arises at the electrode surface when an electrical double layer forms in an electrochemical sensor [46]. Hence DPV approach was used for simultaneous determination carried out in the solution mixture of DA and 5-HT by maintaining a constant concentration of one analyte of the mixture while adjusting another. Figure 7a shows that the concentration of 5-HT (0.05 μM) is kept constant, but the concentration of DA increases from 0.06–0.14 μM. The resulting voltammogram demonstrates a linear increase in the oxidation peak current without causing a shift in the DA oxidation peak potentials or the 5-HT voltammetric response. Similarly, 5-HT increased from 0.04–0.16 μM while maintaining a constant (0.1 μM) DA in the presence of 0.2 M PBS of (pH 7.0) at ADA/MGCE with the sweep rate of 50 mV s<sup>-1</sup> and depicted in Fig. 7b. Due to increased current sensitivity and a lack of background current, the peak current increases rapidly as the concentration of the corre-

**Table 1.** Comparative analytical performance of different modified electrodes for detection of DA

Electrode	Linear range, $\mu\text{M}$	Detection limit, nM	Sensitivity, $\text{mA } \mu\text{M}^{-1} \text{ cm}^2$	Method	References
Poly(EBT) MGCE	0.1–20	20	—	DPV	[38]
ERGO-pEBT/AuNPs/GCE	0.5–5.0	170	—	DPV	[39]
Poly-NBAR modified GCE	5–25	300	—	DPV	[40]
Poly-Evans Blue modified GCE	1–30	250	—	DPV	[41]
NTO NPs/MGCE	0.5–5.0	170	—	DPV	[42]
<b>p-ADA /MGCE</b>	<b>0.01–0.25</b>	<b>1.52</b>	<b>0.22</b>	<b>CV</b>	<b>Present work</b>
<b>p-ADA /MGCE</b>	<b>0.001–0.055</b>	<b>1.9</b>	<b>0.34</b>	<b>DPV</b>	<b>Present work</b>

poly (EBT), polymerized eriochrome black T; ERGO-pEBT/Au NP, electrochemically reduced graphene oxide poly-eriochrome black T/gold nanoparticles; poly-NBAR, poly-nitrobenzenazo resorcinol; NTO NPs, NaTaO<sub>3</sub> nanoparticles.

**Table 2.** Comparative analytical performance of different modified electrodes for detection of 5-HT

Electrode	Linear range, $\mu\text{M}$	Detection limit, nM	Sensitivity, $\text{mA } \mu\text{M}^{-1} \text{ cm}^2$	Method	References
PBBR-MGPE	10–80	310	—	CV	[43]
Poly (FSBF)MPGE	10–50	170	—	CV	[44]
Poly(ser)/MWCNT/GCE	0.1–2000	200	—	DPV	[45]
RGO-Co <sub>3</sub> O <sub>4</sub> /GCE	1–51	48.7	2.2	DPV	[14]
p-NGB/MGCE	10–80	183	—	CV	[4]
<b>p-ADA /MGCE</b>	<b>0.01–1.17</b>	<b>8.9</b>	<b>0.12</b>	<b>CV</b>	<b>Present work</b>
<b>p-ADA /MGCE</b>	<b>0.01–1.15</b>	<b>4.16</b>	<b>0.11</b>	<b>DPV</b>	<b>Present work</b>

PBBR-MGPE, Bismarck brown R-modified graphite pencil electrode; Poly (FSBF)MPGE, poly (Fast sulphone black F) modified pencil graphite electrode; Poly(ser)/MWCNT, poly serine multiwalled carbon nanotube; RGO-Co<sub>3</sub>O<sub>4</sub>, reduced graphene oxide-cobalt oxide nanocomposite; p-NGB, poly-Naphthol Green B.

sponding analyte increases, as can be seen in Figs. 7a and 7b. The oxidation potential of the electroactive biomolecule DA (0.11 V) and 5-HT (0.27 V) is extremely close to each other, as follows from the Figures, the difference in the oxidation potentials between DA and 5-HT is about 160 mV (Samie et al. reported oxidation potentials separated only by 150 mV) [15], which is large enough to determine DA and 5-HT individually and simultaneously at p-ADA/MGCE.

#### Reproducibility, Stability, and Real Sample Analysis

The reproducibility of the electrode was examined in five parallel experiments (5 separate samples). The relative standard deviation was 1.8, and 1.5% for the determination of  $20 \times 10^{-4}$  M DA, and  $80 \times 10^{-4}$  M

5-HT solution ( $n = 10$ ) shown in Fig. SI-4a. To examine the operational stability of p-ADA /MGCE, the sensor was continuously scanned for 10 consecutive cycles using a mixture of solution containing  $20 \times 10^{-4}$  M DA and  $80 \times 10^{-4}$  5-HT in 0.2 M PBS at (pH 7.0) with a sweep rate of  $50 \text{ mV s}^{-1}$  was shown in Fig. SI-4b. As a result of this figure, the electrode retained 96 and 93% of its initial voltammetric response for DA and 5-HT respectively, which confirms the good stability of the electrode. The modified electrode was kept at room temperature for 3 weeks, and tested for stability. The results showed the same shape of the voltammograms (shown in Fig. SI-4c) and the peak currents of two analytes decreased by only 4.0 and 1.4%, indicating that p-ADA/MGCE was highly stable [4, 30, 48].

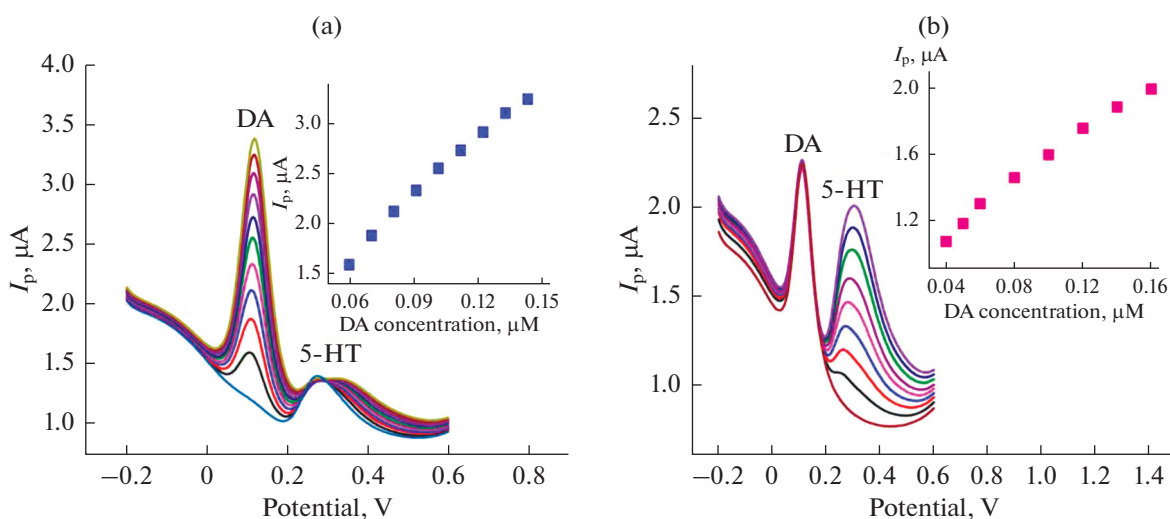


**Fig. 7.** DPVs for different concentrations of DA (0.06–0.14  $\mu\text{M}$ ) in 0.2 M PBS of pH 7 with 0.05  $\mu\text{M}$  5-HT with a Scan rate of 50  $\text{mV s}^{-1}$  at p-ADA/MGCE (a). DPVs of 5-HT (0.04–0.16  $\mu\text{M}$ ) in 0.2 M PBS of pH 7 with 0.1  $\mu\text{M}$  DA with a Scan rate of 50  $\text{mV s}^{-1}$  at p-ADA/MGCE (b).

DA and 5-HT usually coexist in biological fluids, thus the practicability of p-ADA/MGCE in real sample analysis was evaluated with serum and urine as practical samples. All samples were diluted with 0.2 M PBS (pH 7.0) before analysis and transferred to the electrochemical cell for determination. To determine the concentration of DA, and 5-HT using the voltammetric methods described above, the standard addition method was employed. The result obtained is tabulated in Table 3. It was found that p-ADA/MGCE exhibited satisfactory results, indicating that it can be effectively used for the determination of DA and 5-HT in real samples [15, 28, 29, 47].

## CONCLUSIONS

In summary, a simple electropolymerization method has been successfully used to develop an efficient and highly sensitive electrochemical sensor based on the anthraquinone azo dye (ADA) for the simultaneous detection of DA and 5-HT. The electrocatalytic activity of as-prepared p-ADA/MGCE demonstrated excellent results for the oxidation of DA and 5-HT, with detection limits of 1.9 and 4.16 nM, respectively. When DA and 5-HT were determined

simultaneously from serum and urine samples, the novel sensor system exhibited acceptable recovery limits. According to the results, anthraquinone azo dye ADA may find use in the development of an electrochemical sensing platform with enhanced performance.

## SUPPLEMENTARY INFORMATION

The online version contains supplementary material available at <https://doi.org/10.1134/S1023193524700289>.

FT-IR,  $^1\text{H}$  NMR, HRMS spectrum and its spectral data, and Cyclic voltammogram for the stability of electrode.

**Fig. SI-1.** FT-IR spectra of ADA molecule.

**Fig. SI-2.** HR-MS spectra of ADA molecule.

**Fig. SI-3.**  $^1\text{H}$ -NMR spectra of ADA molecule.

**Fig. SI-4.** CVs of five separate samples 0.2  $\mu\text{M}$  DA and 0.8  $\mu\text{M}$  5-HT, in 0.2 M PBS at p-ADA /MGCE with scan rate 50  $\text{mV s}^{-1}$  (a). CVs of 0.2  $\mu\text{M}$  DA and 0.8  $\mu\text{M}$  5-HT in 0.2 M PBS (pH 7) solution for ten continuous cycles (b). CVs of DA and 5-HT by the same p-ADA /MGCE stored in PBS for up to 3 weeks (c).

## FUNDING

The authors greatly acknowledge their work to the Council for Scientific and Industrial Research (CSIR), New Delhi, India, for providing funds for carrying out the research work through a research grant and the award letter number of Senior Research fellowship [09/1207(0566)/2020-EMR-II].

**Table 3.** Determination results of DA and 5-HT in serum and urine samples using p-ADA/MGCE ( $n = 6$ )

Samples		Added, $\mu\text{M}$	Found, $\mu\text{M}$	Recovery, %
Serum	DA	3.0	3.1	103
	5-HT	8.0	7.8	97
Urine	DA	2.5	2.6	104
	5-HT	5.0	5.7	114

## CONFLICT OF INTEREST

The authors of this work declare that they have no conflicts of interest.

## REFERENCES

- Tajik, S., Dourandish, Z., Zhang, K., Beitollahi, H., Van Le, Q., Jang, H.W., and Shokouhimehr, M., Carbon and graphene quantum dots: a review on syntheses, characterization, biological and sensing applications for neurotransmitter determination, *RSC Adv.*, 2020, vol. 10, p. 15406.
- Atta, N.F., Ahmed, Y.M., and Galal, A., Electrochemical determination of neurotransmitters at crown ether modified carbon nanotube composite: application for sub-nano-sensing of serotonin in human serum, *Electroanalysis*, 2018, vol. 31, p. 1204.
- Valsalakumar, V.C., Joseph, A.S., Piyus, J., and Vasudevan, S., Polyaniline-graphene oxide composites decorated with  $ZrO_2$  nanoparticles for use in screen-printed electrodes for real-time l-tyrosine sensing, *ACS Appl. Nano Mater.*, 2023, vol. 6, p. 8382.
- Swamy, B.K. and Ebenso, E., A glassy carbon electrode modulated with Poly (Naphthol green B) for simultaneous electroanalysis of serotonin and Epinephrine in the presence of l-tryptophan, *Inorg. Chem. Commun.*, 2022, vol. 145, 110013.
- Suhito, I.R., Koo, K.M., and Kim, T.H., Recent advances in electrochemical sensors for the detection of biomolecules and whole cells, *Biomedicines*, 2021, vol. 9, p. 1.
- Kaur, H., Siwal, S.S., Saini, R.V., Singh, N., and Thakur, V.K., Significance of an electrochemical sensor and nanocomposites: toward the electrocatalytic detection of neurotransmitters and their importance within the physiological system, *ACS Nanosci. Au.*, 2022, vol. 3, p. 1.
- Yu, H.W., Jiang, J.H., Zhang, Z., Wan, G.C., Liu, Z.Y., Chang, D., and Pan, H.Z., Preparation of quantum dots CdTe decorated graphene composite for sensitive detection of uric acid and dopamine, *Anal. Biochem.*, 2017, vol. 519, p. 92.
- Fang, J., Xie, Z., Wallace, G., and Wang, X., Co-deposition of carbon dots and reduced graphene oxide nanosheets on carbonnanofiber microelectrode surface for selective detection of dopamine, *Appl. Surf. Sci.*, 2017, vol. 412, p. 131.
- Wang, H., Ren, F., Wang, C., Yang, B., Bin, D., Zhang, K., and Du, Y., Simultaneous determination of dopamine, uric acid and ascorbic acid using a glassy carbon electrode modified with reduced graphene oxide, *RSC Adv.*, 2014, vol. 4, p. 26895.
- Zaved, M., Khan, H., Liu, X., Tang, Y., Zhu, J., Hu, W., and Liu, X., A glassy carbon electrode modified with a composite consisting of gold nanoparticle, reduced graphene oxide and poly(L-arginine) for simultaneous voltammetric determination of dopamine, serotonin and L-tryptophan, *Microchim. Acta*, 2018, vol. 185, p. 1.
- Orzari, L.O., Freitas, R.C.D., Andreotti, I.A.D.A., Gatti, A., and Janegitz, B.C.A., Novel disposable self-adhesive inked paper device for electrochemical sensing of dopamine and serotonin neurotransmitters and bio-sensing of glucose, *Biosens. Bioelectron.*, 2019, vol. 138, 111310.
- Lavanya, N. and Sekar, C.,  $\text{SnO}_2-\text{SnS}_2$  nanocomposite as electrocatalyst for simultaneous determination of depression biomarkers serotonin and tryptophan, *J. Electroanal. Chem.*, 2019, vol. 840, p. 1.
- Rejithamol, R., Krishnan, R.G., and Beena, S., Disposable pencil graphite electrode decorated with a thin film of electro-polymerized 2,3,4,6,7,8,9,10-octahydroimidazo [1,2-a] azepine for simultaneous voltammetric analysis of dopamine, serotonin and tryptophan, *Mater. Chem. Phys.*, 2021, vol. 258, 123857.
- Dinesh, B., Veeramani, V., Chen, S.M., and Saraswathi, R., In situ electrochemical synthesis of reduced graphene oxide-cobalt oxide nanocomposite modified electrode for selective sensing of depression biomarker in the presence of ascorbic acid and dopamine, *J. Electroanal. Chem.*, 2017, vol. 786, p. 169.
- Samie, H.A. and Arvand, M.,  $\text{RuO}_2$  nanowires on electrospun  $\text{CeO}_2-\text{Au}$  nanofibers/functionalized carbon nanotubes/graphite oxide nanocomposite modified screen-printed carbon electrode for simultaneous determination of serotonin, dopamine and ascorbic acid, *J. Alloys Compd.*, 2019, vol. 782, p. 824.
- Selvam, S.P. and Yun, K., A self-assembled silver chalcogenide electrochemical sensor based on rGO-Ag<sub>2</sub>Se for highly selective detection of serotonin, *Sens. Actuators B: Chem.*, 2020, vol. 302, 127161.
- Shirane, M. and Nakamura, K., Aniracetam enhances cortical dopamine and serotonin release via cholinergic and glutamatergic mechanisms in SHRSP, *Brain Res.*, 2001, vol. 916, p. 211.
- Ohnuki, Y., Ohsaka, T., Matsuda, H., and Oyama, N., Perm selectivity of films prepared by electrochemical oxidation of phenol and aminoaromatic compounds, *J. Electroanal. Chem.*, 1983, vol. 158, p. 55.
- Volkov, A., Tourillon, G., Lacaze, P.C., and Dubois, J.E., Electrochemical polymerization of aromatic amines: IR, XPS and PMT study of thin film formation on a Pt electrode, *J. Electroanal. Chem.*, 1980, vol. 115, p. 279.
- Lane, R.F. and Blaha, C.D., Detection of catecholamines in brain tissue: surface-modified electrodes enabling *in vivo* investigations of dopamine function, *Langmuir*, 1990, vol. 6, p. 56.
- Ewing, A.G., Dayton, M.A., and Wightman, R.M., Pulse voltammetry with microvoltammetric electrodes, *Anal. Chem.*, 1981, vol. 53, p. 1842.
- Mattson, J.S. and Jones, T.T., Infrared spectrophotometric observations of the adsorption of fibrinogen from solution at optically transparent carbon film electrode surfaces, *Anal. Chem.*, 1976, vol. 48, p. 2164.
- Jin, G., Zhang, Y., and Cheng, W., Poly(p-aminobenzene sulfonic acid)-modified glassy carbon electrode for simultaneous detection of dopamine and ascorbic acid, *Sens. Actuators B: Chem.*, 2005, vol. 107, p. 528.
- Grzeszczuk, M., Polymer electrodes: preparation, properties and applications, in *Encyclopedia of Interfacial Chemistry—Surface Science and Electrochemistry*, Wandelt, K., Ed., Elsevier, 2018, pp. 838–848.
- Yang, T., Yin, H., Gao, L.H., Wang, K.Z., and Yan, D., Chapter seven—recent advances in electrodes modified with ruthenium complexes for electrochemical and photoelectrochemical water oxidation, *Adv. Inorg. Chem.*, 2019, vol. 74, p. 305.

26. Kumar, M., Wang, M., Swamy, B.K., Praveen, M., and Zhao, W., Poly (alanine)/NaOH/MoS<sub>2</sub>/MWCNTs modified carbon paste electrode for simultaneous detection of dopamine, ascorbic acid, serotonin and guanine, *Colloids Surf. B. Biointerfaces*, 2020, vol. 196, 111299.
27. Reddaiah, K., Reddy, T.M., Ramana, D.V., and Rao, Y.S., Poly-Alizarin red S/multiwalled carbon nanotube modified glassy carbon electrode for the boost up of electrocatalytic activity towards the investigation of dopamine and simultaneous resolution in the presence of 5-HT: a voltammetric study, *Mater. Sci. Eng. C*, 2016, vol. 62, p. 506.
28. Mahanthesha, K.R. and Swamy, B.K., Pretreated/carbon paste electrode based voltammetric sensors for the detection of dopamine in presence of ascorbic acid and uric acid, *J. Electroanal. Chem.*, 2013, vol. 703, p. 1.
29. Rezaei, R., Foroughi, M.M., Beitollahi, H., and Alizadeh, R., Electrochemical sensing of uric acid using a ZnO/graphene nanocomposite modified graphite screen printed electrode, *Russ. J. Electrochim.*, 2018, vol. 54, p. 860.
30. Zhu, P. and Zhao, Y., Cyclic voltammetry measurements of electroactive surface area of porous nickel: Peak current and peak charge methods and diffusion layer effect, *Mater. Chem. Phys.*, 2019, vol. 233, p. 60.
31. Mahanthesha, K.R. and Swamy, B.K., Pretreated/carbon paste electrode based voltammetric sensors for the detection of dopamine in presence of ascorbic acid and uric acid, *J. Electroanal. Chem.*, 2013, vol. 703, p. 1.
32. Agarwal, H.P., Influence of indifferent electrolytes on transfer coefficient of Fe(CN)<sub>6</sub>/Fe(CN)<sub>6</sub> system, *J. Electrochem. Soc.*, 1963, vol. 110, p. 237.
33. Vernekar, P.R., Purohit, B., Shetti, N.P., and Chandra, P., Glucose modified carbon paste sensor in the presence of cationic surfactant for mefenamic acid detection in urine and pharmaceutical samples, *Microchem. J.*, 2021, vol. 160, 105599.
34. Gao, J., He, P., Yang, T., Zhou, L., Wang, X., Chen, S., and Liu, J., Electrodeposited NiO/graphene oxide nanocomposite: an enhanced voltammetric sensing platform for highly sensitive detection of uric acid, dopamine and ascorbic acid, *J. Electroanal. Chem.*, 2019, vol. 852, 113516.
35. Kumar, S.A., Tang, C.F., and Chen, S.M., Poly(4-amino-1-1'-azobenzene-3,4'-disulfonic acid) coated electrode for selective detection of dopamine from its interferences, *Talanta*, 2008, vol. 74, p. 860.
36. Rafati, A.A., Afraz, A., Hajian, A., and Assari, P., Simultaneous determination of ascorbic acid, dopamine, and uric acid using a carbon paste electrode modified with multiwalled carbon nanotubes, ionic liquid, and palladium nanoparticles, *Microchim. Acta*, 2014, vol. 181, p. 1999.
37. Devnani, H., Rashid, N., and Ingole, P.P., Copper/cuprous oxide nanoparticles decorated reduced graphene oxide sheetsbased platform for bio-electrochemical sensing of dopamine, *Chem. Select*, 2019, vol. 4, p. 633.
38. Yao, H., Sun, Y., Lin, X., Tang, Y., and Huang, L., Electrochemical characterization of poly (eriochrome black T) modified glassy carbon electrode and its application to simultaneous determination of dopamine, ascorbic acid and uric acid, *Electrochim. Acta*, 2007, vol. 52, no. 20, p. 6165.
39. Edris, N.M.M.A., Abdullah, J., Kamaruzaman, S., Saiman, M.I., and Sulaiman, Y., Electrochemical reduced graphene oxide-poly (eriochrome black T)/gold nanoparticles modified glassy carbon electrode for simultaneous determination of ascorbic acid, dopamine and uric acid, *Arab. J. Chem.*, 2018, vol. 11, p. 1301.
40. Lin, X., Zhang, Y., Chen, W., and Wu, P., Electrocatalytic oxidation and determination of dopamine in the presence of ascorbic acid and uric acid at a poly (p-nitrobenzenazo resorcinol) modified glassy carbon electrode, *Sens. Actuators B: Chem.*, 2007, vol. 122, p. 309.
41. Lin, L., Chen, J., Yao, H., Chen, Y., Zheng, Y., and Lin, X., Simultaneous determination of dopamine, ascorbic acid and uric acid at poly (Evans Blue) modified glassy carbon electrode, *Bioelectrochemistry*, 2008, vol. 73, p. 11.
42. Pallavi, K.M., Mamatha, G.P., Nagaraju, G., and Soundarya, T.L., Facile synthesis of NaTaO<sub>3</sub> for detection of dopamine, *Inorg. Chem. Commun.*, 2023, vol. 158, 111427.
43. Swamy, B.K. and Ebenso, E., Voltammetric analysis of serotonin and epinephrine in the presence of guanine and adenine at Bismarck brown R amplified pencil graphite electrode, *Inorg. Chem. Commun.*, 2022, vol. 144, 109868.
44. Banu, R., Swamy, B.K., and Deepa, S., Poly (fast sulphone black F) modified pencil graphite electrode sensor for serotonin, *Sens. Int.*, 2020, vol. 1, 100044.
45. Narayana, P.V., Reddy, T.M., Gopal, P., Reddy, M.M., and Naidu, G.R., Electrocatalytic boost up of epinephrine and its simultaneous resolution in the presence of serotonin and folic acid at poly (serine)/multi-walled carbon nanotubes composite modified electrode: a voltammetric study, *Mater. Sci. Eng. C*, 2015, vol. 56, p. 57.
46. Manivel, P., Dhakshnamoorthy, M., Balamurugan, A., Ponpandian, N., Mangalaraj, D., and Viswanathan, C., Conducting polyaniline-graphene oxide fibrous nanocomposites: preparation, characterization and simultaneous electrochemical detection of ascorbic acid, dopamine and uric acid, *RSC Adv.*, 2013, vol. 3, p. 14428.
47. Hasanzadeh, M., Shadjou, N., and Omidinia, E., A novel electroanalytical method for simultaneous detection of two neurotransmitter dopamine and serotonin in human serum, *J. Neurosci. Methods*, 2013, vol. 219, p. 52.
48. Nemakal, M. and Sannegowda, L.K., *Sens. Actuators A: Phys.*, 2021, vol. 324, p. 112690.  
<https://doi.org/10.1016/j.sna.2021.112690>

**Publisher's Note.** Pleiades Publishing remains neutral with regard to jurisdictional claims in published maps and institutional affiliations.